

Experimental study of $\bar{K}NN$ and future experiments for kaonic nuclei

Takumi Yamaga^{1,*} for the J-PARC E15, E80, and P89 collaborations

¹RIKEN Cluster for Pioneering Research, RIKEN, Wako, 351-0198, Japan

Abstract. Quasi-bound systems of antikaon and nucleus, \bar{K} -nuclei, have been considered as a natural extension of the interpretation that $\Lambda(1405)$ is the \bar{K} -N hadronic molecule. The lightest \bar{K} -nucleus, $\bar{K}NN$ quasi-bound state, is particularly important to be investigated for confirmation of the existence of such an exotic nuclear state containing a meson. We conducted an experiment, J-PARC E15, to search for $\bar{K}NN_{(I_z=+1/2)}$ by the in-flight K^- induced reaction on ^3He , and finally observed a clear signal of $\bar{K}NN_{(I_z=+1/2)}$ for the first time. To robustly confirm the existence of \bar{K} -nuclei, we have planned systematic measurements for various \bar{K} -nuclei at J-PARC.

1 Introduction

The kaonic nucleus is a quasi-bound system containing antikaon (\bar{K}) and nucleons (N). The existence of such an exotic nuclear state, which has a meson as a building block, was predicted as a natural extension of the interpretation of $\Lambda(1405)$ being \bar{K} -N hadronic molecule due to the strong attractive $\bar{K}N$ interaction in isospin $I_{\bar{K}N} = 0$ channel rather than simple three quark state. Many theoretical studies for kaonic nuclei have been done since the $\bar{K}N$ interaction was established to be strongly attractive by measuring X -ray from kaonic hydrogen. All those theoretical works support the existence of kaonic nuclei, although predicted binding energies and decay widths are widely distributed which is due to the energy dependence of $\bar{K}N$ interaction in their models.

After the first detailed theoretical calculation for kaonic nuclei [1, 2], several experiments have been performed to search for kaonic nuclei, especially for the lightest system, $\bar{K}NN$. Considering the probability of $I_{\bar{K}N} = 0$ component in the system, $\bar{K}NN$ would be isospin $I = 1/2$ with spin and parity of $J^\pi = 0^-$. Thus, most experiments searched for $\bar{K}NN$ by its non-mesonic decay mode of $\bar{K}NN \rightarrow \Lambda N$. Because of experimental difficulty in the detection of neutral particles, experimental searches focused on $\bar{K}NN$ with $I_z = +1/2$ state, which has a positive charge so decays as $\bar{K}NN_{(I_z=+1/2)} \rightarrow \Lambda p \rightarrow (\pi^- p)p$.

Searches for $\bar{K}NN_{(I_z=+1/2)}$ were performed with various reaction processes: pp collisions [3, 4], γ induced [5], π^+ induced [6], and stopped- K^- induced [7, 8] reactions. In the stopped- K^- induced reactions, the K^- is bound to NN in a light nucleus target, such as Li or C, by releasing extra energy, corresponding to binding energy, into residual nucleons. In the other reaction processes not using K^- -beam, the K^+K^- pair creation process is expected to be the source of \bar{K} . Some of those works observed candidates of $\bar{K}NN_{(I_z=+1/2)}$ signal [3, 6, 7],

* e-mail: takumi.yamaga@riken.jp

while some of those reported null results [4, 5, 8]. Thus, the existence of $\bar{K}NN$ was not established with those works.

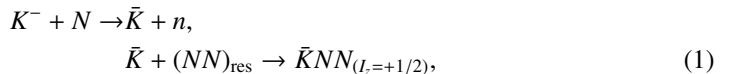
The most severe problem in those experiments is that there are many background channels to contaminate the spectrum. For instance, in the stopped- K^- induced experiment, the multi-nucleon absorption of K^- is the major background that overlaps with the $\bar{K}NN$ signal. In the K^+K^- pair creation experiments, the main background is the $K^+\Lambda$ or $K^+\Sigma$ production by converting a proton to the hyperon that needs smaller energy than the K^+K^- pair. Thus, although they tagged the K^+ production, the existence of intermediate- \bar{K} is not secured.

To search for $\bar{K}NN_{(I_z=+1/2)}$, we performed the J-PARC E15 experiment. We utilized the in-flight (K^-, n) reaction to effectively produce $\bar{K}NN_{(I_z=+1/2)}$, suppress background processes, and easily isolate the signal from background contaminations. The produced $\bar{K}NN_{(I_z=+1/2)}$ state is reconstructed by its non-mesonic decay mode, $\bar{K}NN_{(I_z=+1/2)} \rightarrow \Lambda p$. From the exclusive measurement for the $K^- {}^3\text{He} \rightarrow \Lambda p n$ reaction, we finally observed a distinct peak in the Λp invariant-mass spectrum which is interpreted as a signal of $\bar{K}NN_{(I_z=+1/2)}$ [9, 10].

In this paper, we review the result of J-PARC E15 and overview future projects to investigate \bar{K} nuclei at J-PARC. In Sec. 2, we briefly introduce the J-PARC E15 experiment and the production of $\bar{K}NN_{(I_z=+1/2)}$ in the (K^-, n) reaction. In Sec. 3, we show the analysis result of the $K^- {}^3\text{He} \rightarrow \Lambda p n$ reaction. The future projects for further investigation of \bar{K} -nuclei is described in Sec. 4.

2 J-PARC E15

We measured an in-flight K^- induced reaction on the helium-three target, the $K^- + {}^3\text{He} \rightarrow \Lambda p n$ reaction, to search for $\bar{K}NN_{(I_z=+1/2)}$ by its non-mesonic decay mode, $\bar{K}NN_{(I_z=+1/2)} \rightarrow \Lambda p$. Thus, we selected the $\Lambda p n$ final state and measured the invariant mass of the Λp system. We chose the incident K^- -beam momentum of 1 GeV/c, at which the reaction cross-section of elementary reactions, $K^-N \rightarrow \bar{K}n$, is maximized corresponding Y^* -resonances located ~ 1.8 GeV. Because of the large $K^-N \rightarrow \bar{K}n$ cross-section, the reaction process could be considered as a cascade reaction:



where $(NN)_{\text{res}}$ denotes residual nucleons in the first reaction. In the first step reaction, the induced K^- -beam knocks out a neutron and is recoiled back by decreasing its momentum to a minimum ~ 0.2 GeV/c at the small neutron emission angle. Due to the small recoil momentum, it is expected that the intermediate- \bar{K} is effectively absorbed by the two residual nucleons. Therefore, the production cross-section of $\bar{K}NN_{(I_z=+1/2)}$ would be rather large although the induced K^- -beam originally has a rather large momentum.

The reaction process,



can be characterized by two kinematical parameters, the invariant mass of X (m_X) and the momentum transfer to X (q_X). If we assume that the reaction process is the cascade reaction described in Eq. 1, m_X and q_X correspond to the invariant-mass of $\bar{K}+(NN)_{\text{res}}$ and the momentum of the intermediate- \bar{K} , respectively. Thus, we analyzed a two-dimensional distribution on the (m_X, q_X) plane.

The experiment was performed at the K1.8BR beamline of the hadron experimental facility at J-PARC in 2015. A high-intensity secondary K^- -beam is produced by bombarding a

gold target with a 30 GeV primary proton beam. The K^- beam is identified and measured its momentum by a beamline spectrometer system at the K1.8BR beamline. An experimental target, liquid ^3He , is located at the final focal plane of the beamline. The K^- -beam is induced into the ^3He target, and particles generated in the reaction are detected by a cylindrical detector system (CDS), which surrounds the target. CDS is composed of a cylindrical drift chamber for tracking and a cylindrical detector hodoscope for a time-of-flight measurement. The detectors are installed inside a solenoid magnet providing a magnetic field along the K^- beam direction of which field strength is 0.7 T. More detailed information on the detector system can be found in Ref. [11].

In the analysis, we selected events of the $\Lambda p n$ final state and measured a two-dimensional distribution of the Λp invariant mass and the momentum transfer to Λp for the selected events. To select the $\Lambda p n$ final state, we required that three charged particles, $p p \pi^-$, are detected with CDS. Among the two $p \pi^-$ pairs in the detected $p p \pi^-$, the $\Lambda \rightarrow p \pi^-$ candidate is chosen by the invariant mass of a pair and distances of the closest approach between charged tracks (DCA). The neutron in the final state is not detected with CDS but is kinematically identified by the kinematical fit. The final events of the $\Lambda p n$ final state are selected based on a log-likelihood function containing χ^2 of the kinematical fit and DCA information. The analysis procedure is described in more detail in Ref. [10]. The number of selected events is ~ 6000 with the integrated luminosity of 2.9 nb^{-1} while the contamination ratio is evaluated to be $\sim 20\%$ which mainly comes from the wrong identification of $\Sigma^0 p n$ and $\Sigma^- p p$ final states as the $\Lambda p n$ final state.

3 Observation of $\bar{K}NN_{(I_z=+1/2)}$

For the selected $\Lambda p n$ final state events, we measured a two-dimensional distribution on the invariant mass of Λp pair (m_X) and the momentum transfer to the pair (q_X) as shown in Fig. 1. To obtain the double differential cross-section $d^2\sigma/(dm_X dq_X)$, we corrected the acceptance containing the geometrical acceptance, the detection efficiency of CDS, and the analysis efficiency. In the correction, we ignored small sensitivity regions having an acceptance of less than 5%, which is indicated by gray hatched in the figure, to ensure the reliable correction.

There are three clear events-concentrations in the figure. One is located at m_X below the mass threshold of an antikaon and two nucleons system ($m_{\bar{K}} + 2m_N$), indicated by the gray vertical dotted line in the figure. The two events-concentrations are situated above the threshold; they are distributed along the blue dotted curve in the figure, which is described by

$$M_F(q_X) = \sqrt{4m_N^2 + m_{\bar{K}}^2 + 4m_N \sqrt{m_{\bar{K}}^2 + q_X^2}}. \quad (3)$$

Equation 3 is nothing but the invariant mass of antikaon having the momentum of q_X and two nucleons at rest. Therefore, the two events-concentrations can be interpreted as quasi-free \bar{K} absorption into two nucleons, in which the intermediate- \bar{K} having almost on-shell mass is absorbed by the residual two nucleons having Fermi momentum. On the other hand, the events-concentration below the mass threshold is well separated from the quasi-free events, and its m_X centroid does not change in different q_X -region. Thus, the events concentration should be produced by any resonance state, so it could be a signal of $\bar{K}NN_{(I_z=+1/2)}$.

To isolate a signal of $\bar{K}NN_{(I_z=+1/2)}$, we conducted a model fitting for the obtained two-dimensional distribution. We considered the following three processes in our model: (K) the $\bar{K}NN_{(I_z=+1/2)}$ production process, (F) the quasi-free \bar{K} absorption process, and (B) a broad component. The two dimensional distributions of the processes (K) and (F) are shown in Fig. 2(a) and (b). The broad distribution (B) is produced by a quasi-free \bar{K} absorption process

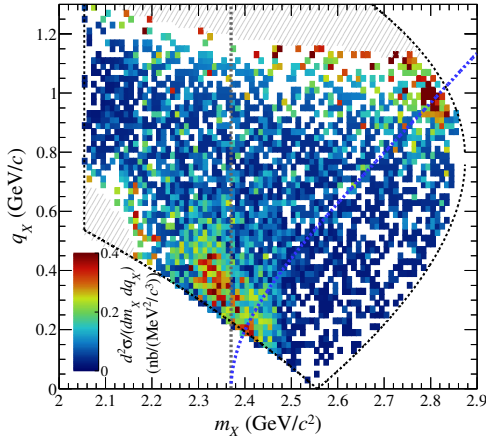


Figure 1. Two-dimensional distribution of the invariant mass of Δp pair (m_X) and the momentum transfer to the pair (q_X). The black dotted lines show the kinematical limit in the reaction. The gray dotted line is the mass threshold of $m_K + 2m_N$. The blue dotted curve shows the kinematical line of the quasi-free reaction. (See the text for more details.) The figure was taken from Ref. [10].

if a proton (not a neutron) is knocked out in the first step elementary reaction described in Eq. 1. In the quasi-free process with a proton knocked out, the second step reaction, the \bar{K} absorption process, is described as,

$$K^- + (pn)_{\text{res}} \rightarrow \Lambda n, \quad (4)$$

thus the same two-dimensional distribution as the process (F) (Fig. 2(b)) is observed in a two-dimensional distribution for the Λn system. Instead, the Δp system should not have any correlations between m_X and q_X , so it results in a broad distribution on the present two-dimensional distribution. We introduced a model function for the process (B) rather phenomenologically as the Breit-Wigner formula with a large width as shown in Fig. 2(c). More detailed information for the model functions is described in Ref. [10].

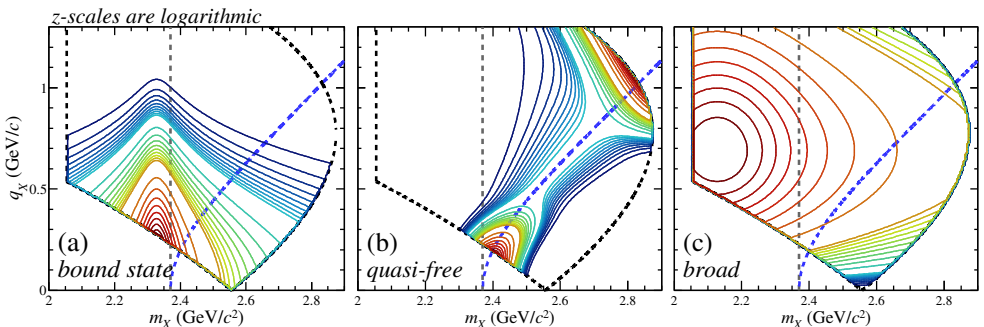


Figure 2. Two-dimensional distribution of model functions for the fit: (a) the $\bar{K}NN_{(l_z=+1/2)}$ production process, (b) the quasi-free \bar{K} absorption process, and (c) the broad component. See the text for more details. The figure was taken from Ref. [10].

Figure 3 shows the fit result on the m_X distributions by selecting various q_X regions. As shown in the figure, the overall distributions are well reproduced by the model functions and background contaminations from $\Sigma^0 pn$ and $\Sigma^- pp$ final states. We obtained the mass and width of the observed state to be $2.328 \pm 0.003(\text{stat.})^{+0.004}_{-0.003}(\text{syst.})$ GeV/c^2 and $100 \pm 7(\text{stat.})^{+19}_{-9}$ (syst.) MeV, respectively, so the observed state has a smaller mass than the $(\bar{K} + 2N)$ mass threshold. Additionally, the existence of intermediate- \bar{K} during the reaction is clear because the quasi-free \bar{K} absorption process is seen. Therefore, we interpreted the observed state as the $\bar{K}NN_{(I_z=+1/2)}$ quasi-bound state. The binding energy of $\bar{K}NN_{(I_z=+1/2)}$, mass reduction from the $(\bar{K} + 2N)$ mass threshold, was obtained to be $42 \pm 3(\text{stat.})^{+3}_{-4}(\text{syst.})$ MeV, which is consistent with some theoretical predictions [12–16].

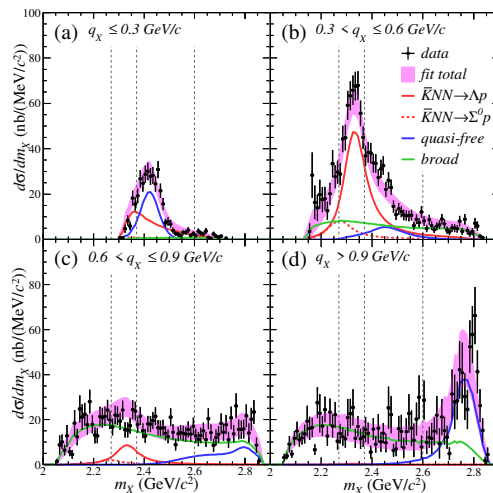


Figure 3. m_X spectra with various q_X intervals with the fit result. The figure was taken from Ref. [10].

On the other hand, the obtained decay width is relatively larger than theoretical predictions which are around 50 MeV. It is also larger than the decay width of $\Lambda(1405)$, which is considered as $\bar{K}N$ hadronic molecule decaying into $\pi\Sigma$ with 100%. A possible explanation of the large decay width of observed $\bar{K}NN_{(I_z=+1/2)}$ is the multi-nucleon absorption of \bar{K} . Indeed, the multi-nucleon absorption is not taken into account in the theoretical calculations. A theoretical calculation suggested that such multi-nucleon absorption could increase the total width by ~ 30 MeV [17]. Thus, we need to measure mesonic decay channels to clarify that possibility. Another possibility is the existence of sub-structure(s) around the $\bar{K}NN_{(I_z=+1/2)}$ signal region, *e.g.*, $\bar{K}NN_{(I_z=+1/2)}$ having $J^\pi = 1^-$, which is predicted as a shallow bound system by a theoretical calculation [18]. To conclude such possibilities, higher statistical data for the same reaction is essential which allows us to decompose the spectra with more detailed model functions.

We interpreted the observed resonance located at m_X below the $(\bar{K} + 2N)$ mass threshold as $\bar{K}NN_{(I_z=+1/2)}$; however, there are other candidates which could contribute to the obtained spectrum, *i.e.*, resonances which satisfy conservations, namely having strangeness $S = -1$ and baryon number $B = 2$, such as Y^*N . Even if those candidates can be excluded, we should clarify whether \bar{K} keeps its particle identity in the system. For those confirmations, systematic measurements for \bar{K} -nuclei are desired, thus we have planned future projects of \bar{K} -nuclei experiments at J-PARC.

4 Future projects

The main goals of the future projects of \bar{K} -nuclei experiments at J-PARC are to robustly confirm the existence of \bar{K} -nuclei and to clarify their internal structures. For those purposes, we consider two directions of the experimental approach. One direction is a more precise measurement for $\bar{K}NN$. Another direction is a systematic measurement for several \bar{K} -nuclei systems having different A .

In the E15 experiment, we found that the in-flight K^- induced reaction is promising to produce \bar{K} -nuclei and isolate its signal from the background contaminations. Thus, the J-PARC hadron experimental facility is a unique and suitable place to investigate \bar{K} -nuclei further. We will construct a new large cylindrical detector system, the conceptual design of which is as shown in Fig. 4, and replace the CDS used in the E15 experiment with the new CDS to conduct future experiments.

The new CDS has approximately twice larger solid angle coverage than the previous CDS, so it can reconstruct many body decay channels of \bar{K} -nuclei with sufficient reconstruction efficiency. Neutrons can also be detected by the new CDS with a plastic scintillator array of which thickness is 15 cm in total. By installing trackers in between layers of the plastic scintillator array, we can measure the proton polarization from proton scattering inside the plastic scintillator. We can perform the systematic measurements for various \bar{K} -nuclei just by replacing the target material with the suitable one, *e.g.*, ^4He to measure $\bar{K}NNN$ system.

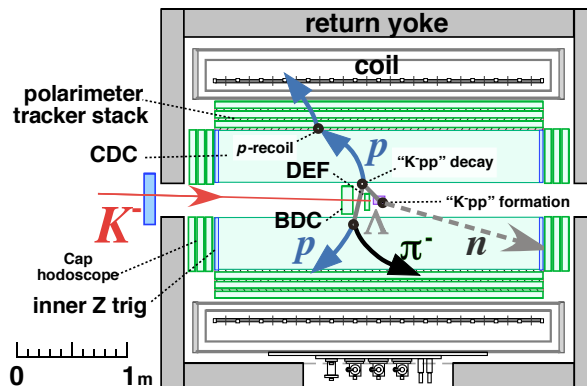


Figure 4. Conceptual design of the new cylindrical detector system.

As the first-step experiments of future projects, we proposed two experiments for the J-PARC PAC: the J-PARC E80 to measure $\bar{K}NNN$ [20], and the J-PARC P89 to measure $\bar{K}NN$ precisely [21]. After conducting those experiments, we will perform further measurements not only for heavier \bar{K} -nuclei than $\bar{K}NNN$ but also for the lighter system, $\Lambda(1405) \equiv \bar{K}N$. We describe those future experiments briefly in the following sections.

4.1 J-PARC E80

The experiment aims to search for the second lightest \bar{K} -nuclue, $\bar{K}NNN$, by the $^4\text{He}(K^-, n)$ reaction. $\bar{K}NNN$ is considered to be $I = 0$ with $J^\pi = 1/2^-$, so it is essential to measure $\bar{K}NNN \rightarrow \Lambda d$ non-mesnoic two-body decay to establish its isospin state. We will also measure three-body decay, $\bar{K}NNN \rightarrow \Lambda pn$, by detecting a neutron with new CDS. From the decay ratio between two- and three-body decay modes, we may extract information on the

internal configuration of $\bar{K}NNN$. We can also measure mesonic decay modes, $\bar{K}NNN \rightarrow \pi YNN$.

4.2 J-PARC P89

The primary purpose of the experiment is to determine J^π of $\bar{K}NN$. The determination of J^π is essential for establishing the observed state as a quantum state and clarifying its internal configuration. To this end, we will measure the spin-spin correlation between Λ and p from $\bar{K}NN_{(I_z=+1/2)} \rightarrow \Lambda p$ decay. Because J^π of initial $\bar{K}NN_{(I_z=+1/2)}$ are conserved during the strong decay, the initial J^π information should appear as spin alignment of Λp system. Therefore, we can determine J^π of $\bar{K}NN$ from the spin alignment measurement in a model-independent way. For this purpose, the proton polarimeter system of the new CDS is essential to measure the proton spin direction while the Λ spin direction can be obtained rather easily from decay asymmetry in the $\Lambda \rightarrow p\pi^-$ decay.

Another purpose is to search for $\bar{K}NN_{(I_z=-1/2)}$, which must exist if $\bar{K}NN_{(I_z=+1/2)}$ exists, by its non-mesonic decay mode $\bar{K}NN_{(I_z=-1/2)} \rightarrow \Lambda n$. Thus, we will measure the ${}^3\text{He}(K^-, p)$ reaction going to the $\Lambda n + p$ final state.

4.3 Other perspectives

We intend to measure $d(K^-, n)$ reaction and reconstruct $\Lambda(1405)$ from $\Lambda(1405) \rightarrow \pi^\pm \Sigma^\mp$ decay by detecting a neutron from $\Sigma^\mp \rightarrow n\pi^\mp$ decay. If we replace the plastic scintillator arrays with an electromagnetic calorimeter to detect γ -rays, it will be possible to reconstruct $\Lambda(1405) \rightarrow \pi^0 \Sigma^0$ decay mode, which is a particularly interesting channel because it contains only the $I = 0$ contribution. However, this measurement should be a long-term project because of the difficulty to construct a large electromagnetic calorimeter.

On the other hand, for heavier systems than $\bar{K}NNN$, experimental difficulties are expected to arise. One of the difficulties is that decay products of heavier \bar{K} -nuclei contain light nuclei, α or heavier, and will need a dedicated detector setup. Another difficulty is that natural width may be getting larger in heavier \bar{K} -nuclei since multinucleon-absorption of \bar{K} may increase in the many-body system. Nevertheless we have planned to measure some heavier \bar{K} -nuclei, e.g., $\bar{K}NNNN$.

$\bar{K}NNNN$ is considered to be $I = 1/2$ with $J^\pi = 0^-$ state, ineternal structure of which would be $K^- \alpha$ for $I_z = -1/2$ and $\bar{K}^0 \alpha$ for $I_z = +1/2$ [19]. Because there is no stable nuclear target with $A = 5$, we will utilize the ${}^6\text{Li}(K^-, d)$ reaction to produce $\bar{K}NNNN$, so the $I_z = -1/2$ state will be measured. Though the in-flight K^- induced reaction is an efficient reaction to measure \bar{K} -nuclei, it would be challenging to measure $\bar{K}NNNN$ because the (K^-, d) reaction has a smaller cross-section than the (K^-, N) reactions, and the momentum transfer in the (K^-, d) reaction is larger than that in the (K^-, N) reaction. Therefore, it is essential for realization of $\bar{K}NNNN$ search to measure production cross sections of $\Lambda(1405)$ and $\bar{K}NN$ with ${}^3\text{He}(K^-, d)$ and ${}^4\text{He}(K^-, d)$ reactions, respectively, in the preceding experiments. Sensitivities for other \bar{K} -nuclei with the in-flight K^- induced reaction and the new CDS are under consideration.

5 Summary

We reviewed the result obtained by the J-PARC E15 experiment, the observation of $\bar{K}NN_{(I_z=+1/2)}$ in the in-flight K^- reaction on ${}^3\text{He}$. A clear signal of $\bar{K}NN_{(I_z=+1/2)}$ was observed in the non-mesonic decay channel, $\bar{K}NN_{(I_z=+1/2)} \rightarrow \Lambda p$ for the first time, and the

binding energy and decay width were obtained from the analysis. However, there are remaining questions, especially for the internal structure of \bar{K} -nuclei. Thus, we have planned further experiments to robustly confirm the existence of \bar{K} -nuclei and to clarify their internal structure. We will conduct systematic measurements for various \bar{K} -nuclei, from $\Lambda(1405) \equiv \bar{K}N$ to $\bar{K}NNNN$, with a newly constructed large cylindrical detector system. The construction of the new detector system has been started in 2022 and will be completed in 2025. Thus, we expect the first measurement to start in 2026.

References

- [1] T. Yamazaki and Y. Akaishi, Phys. Lett. B **535**, 70 (2002)
- [2] Y. Akaishi and T. Yamazaki, Phys. Rev. C **65**, 044005 (2002)
- [3] T. Yamazaki *et al.*, Phys. Rev. Lett. **104**, 132502 (2010)
- [4] G. Agakishiev *et al.*, Phys. Lett. B **742**, 242 (2015)
- [5] A. O. Tokiyasu *et al.*, Phys. Lett. B **728**, 616 (2014)
- [6] Y. Ichikawa *et al.*, Prog. Theor. Exp. Phys. **2015**, 021D01 (2015)
- [7] M. Agnello *et al.*, Nucl. Phys. A **914**, 310 (2013)
- [8] O. Vázquez Doce *et al.*, Phys. Lett. B **758**, 134 (2016)
- [9] S. Ajimura *et al.*, Phys. Lett. B **789**, 620 (2019)
- [10] T. Yamaga *et al.*, Phys. Rev. C **102**, 044002 (2020)
- [11] K. Agari *et al.*, Prog. Theor. Exp. Phys. **2012**, 02B011 (2012)
- [12] T. Yamazaki and Y. Akaishi, Phys. Rev. C **76**, 045201 (2007)
- [13] K. Ikeda and T. Saito, Phys. Rev. C **76**, 035203 (2007)
- [14] K. Ikeda and T. Saito, Phys. Rev. C **79**, 035201 (2009)
- [15] S. Wycech and A. M. Green, Phys. Rev. C **79**, 035201 (2009)
- [16] J. Révai and N. V. Shevchenko, Phys. Rev. C **90**, 034004 (2014)
- [17] M. Bayar and E. Oset, Phys. Rev. C **88**, 044003 (2013)
- [18] N. V. Shevchenko, Few-Body Syst. **61**, 27 (2020)
- [19] S. Ohnishi *et al.*, Phys. Rev. C **95**, 065202 (2017)
- [20] F. Sakuma *et al.*, Proposal for J-PARC E80, https://j-parc.jp/researcher/Hadron/en/pac_2007/pdf/P80_2020-10.pdf
- [21] T. Yamaga *et al.*, Proposal for J-PARC P89, https://j-parc.jp/researcher/Hadron/en/pac_2107/pdf/P89_2021-09.pdf